

# Mission Report

**Project:** Invasive Aquatic Vegetation Assessment

**Location:** Fisheating Bay, Lake Okeechobee, Florida

**Release Date:** October 11<sup>th</sup>, 2010

**Document Status:** *Pre-release*

**Submitted to:** UAS Program - Operations Division  
*U.S. Army Corps of Engineers, Jacksonville District*

**Prepared by:** UAS Research Program  
*University of Florida*

# Contents

---

Summary .....	3
Timeline .....	3
Personnel .....	3
Phase 1 .....	4
Data Acquisition .....	4
Flight Plan .....	4
Equipment .....	4
Data Set .....	5
Resources .....	5
Data Processing .....	6
Preparation .....	6
Results .....	7
Data Analysis .....	11
Summary .....	11
Phase 2 .....	13
Data Acquisition .....	13
Flight Plan .....	13
Equipment .....	13
Data Set .....	14
Resources .....	15
Data Processing .....	16
Preparation .....	16
Results .....	16
Data Analysis .....	17
Summary .....	17

## Summary

---

The UAS Program was commissioned to collect 5 cm GSD aerial orthomosaics of a 0.25 km<sup>2</sup> target area designated by the USACE before and after scheduled herbicidal treatments. This area is known to contain several species of invasive vegetation and was selected by Operations Division personnel. To support the aerial identification of the target species, a random sample of ten points within the target area were ground-truthed for vegetation composition. This report presents the results of the mission in two phases.

## Timeline

---

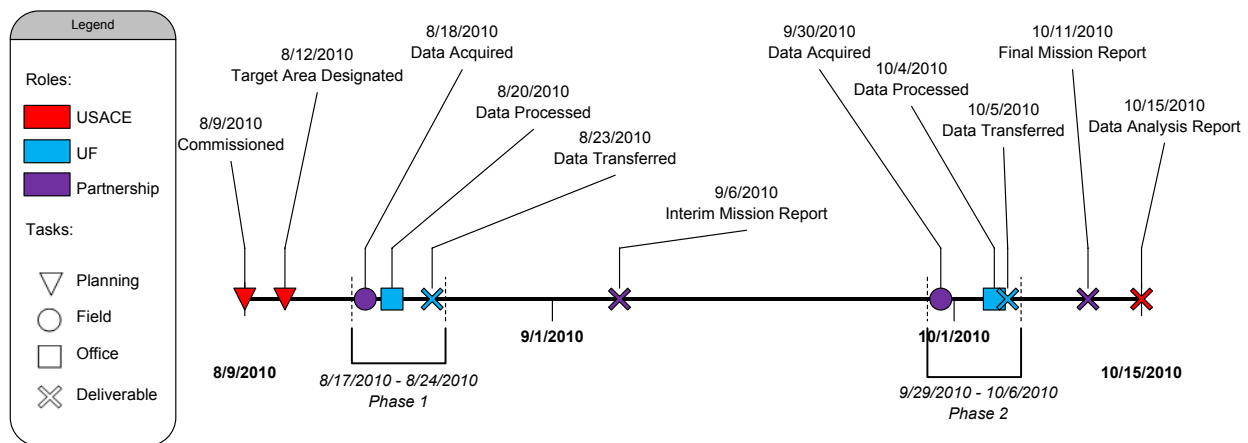


**Figure 1.** *Fisheating Bay Assessment Project Timeline*

## Personnel

---

USACE:

Project Supervisor: Larry Taylor; Data Analyst: Jon Lane; Geodesist: Damon Wolfe; Field Crew: John Morton, Kristen Farmer

UF:

Principal Investigators: H. Franklin Percival, Peter Ifju, Scot Smith, Bon Dewitt; Project Coordinator: Matthew Burgess; Field Crew: Brandon Evers, John Perry, Thomas Rambo, Thomas Reed

# Phase 1

---

## DATA ACQUISITION

### *Flight Plan*

On August 18, 2010, a panchromatic payload flight was conducted at 200 m altitude over a 0.25 km<sup>2</sup> square vegetated plot and its surroundings. The target area was part of Fisheating Bay, located on the western shore of Lake Okeechobee, Florida. Target area selection was performed by Jon Morton, including a pre-flight visit. The site selection criteria was an area representative of the density and species diversity of the Fisheating Bay invasive vegetation. Flight planning was conducted by Matthew Burgess using a modified dipole pattern, with upwind flight lines covering the target area to specification for full 3D coverage. The coordinates of the target were:

CENTROID: 26° 58.506'N, 81° 4.502'W

NE: 26° 58.639'N, 81° 4.358'W

NW: 26° 58.641'N, 81° 4.662'W

SW: 26° 58.365'N, 81° 4.655'W

SE: 26° 58.367'N, 81° 4.353'W

Following flight operations, ten ground-truthing points were visited to classify nearby vegetation species. Species were identified, and roughly quantified by percentage in the immediate surroundings for each of the points. Point locations were selected by a random sampling of the target area polygon, conducted by John Perry. Plant identification was performed by Jon Morton and the location of the randomly selected points were recovered using a handheld Garmin GNSS unit.

### *Equipment*

The data were captured using the U.S. Army Corps of Engineers' NOVA 2.1 UAS platform, configuration #1032. The imaging sensor was an Olympus E-420 dSLR camera, serial #G20519872, with a Zuiko 25mm lens, serial #292029187. The navigation system was the Xsens MTi-G integrated GPS/INS, serial #00500702, with Antcom antenna model #1G1215A-18NRS-4, serial #194292. Sensor synchronization was provided by the Burredo v4, serial #02.

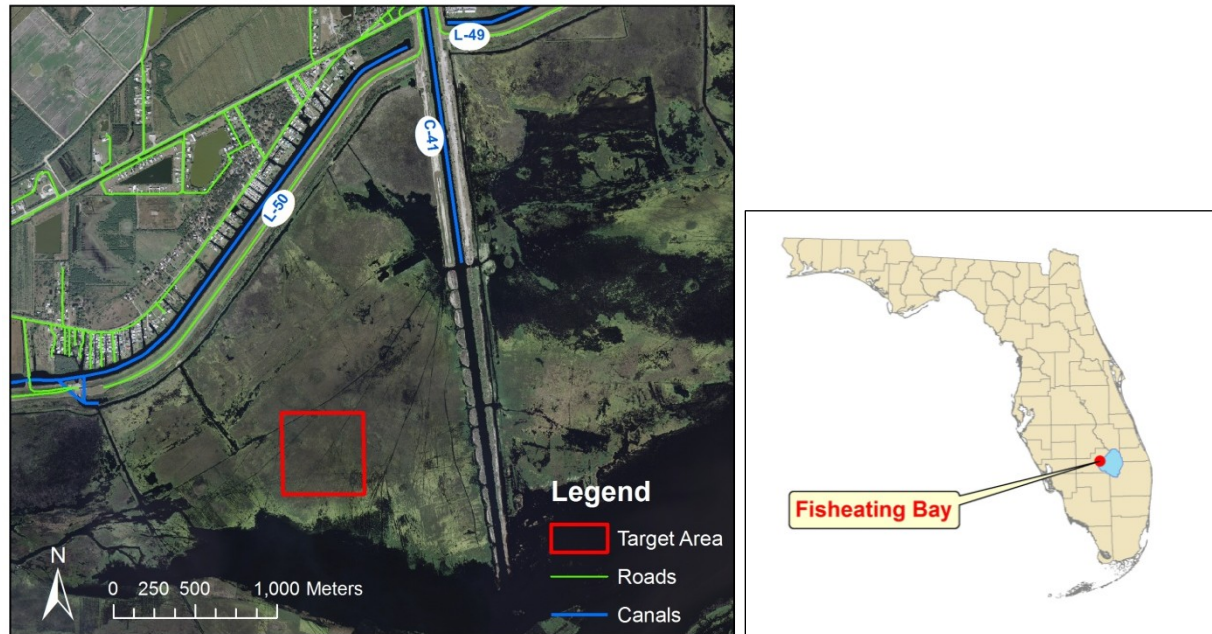


**Figure 2.** *Target vicinity map*

#### *Data Set*

The data acquisition flight time was 9:21 AM – 10:03 AM, and total duration over the target area was 13.2 minutes. The dataset ID# is 01-01-2008-00-14-56. A total of 1009 images were captured during the flight, yielding 3.96 GB of data. Images were recorded at a resolution of 3648 by 2736 (9.98 megapixels) with 8 bit per channel RGB using JPEG compression. Exposures were 1/2000<sup>th</sup> speed, f-stop 2.8, and ISO-100. Nominal focal length was 25mm, with a nominal forward and side field of view of 40° and 30°, respectively. Nominal flight line spacing was 50m, with a 95% confidence interval of  $\pm 3.9$  meter horizontal deviation and  $\pm 2.7$  meter vertical deviation from the flight line. Mean airbase was 36.4 m between adjacent photographs along the flight line, yielding a mean exposure interval of 2.25 seconds. Notable delays in the exposure interval were highly correlated to open water, and indicate the inability of the automatic focusing and metering system to properly function over featureless terrain. Nominal altitude was 200m, with a mean altitude of 190.3 m. The foregoing values were calculated using post-processed exterior orientation parameters.

#### *Resources*

Data processing was performed by John Perry for the two days following the mission. The ratio of data acquisition time to processing time was 1:72, including unattended compute time. This figure was obtained by defining acquisition duration as the time spent over the target area. Approximately 6 hours (30%) of the processing time required manual input from the operator. Given the unrefined workflow, this figure can be expected to improve with further experience.

The following software packages were used to process the data. The Leica Photogrammetry Suite (LPS) from ERDAS, Inc., including the auxillary software modules for terrain extraction, radiometric correction, and mosaicing, were used for the photogrammetry stages of the workflow. ArcGIS from ESRI, Inc. was used to interactively subset the data during the preprocessing stages, and the output of the processing workflow was targeted for this platform. Statistical and geometric analysis of the processing results was performed using Microsoft Excel and MatLAB from The Mathworks, Inc.

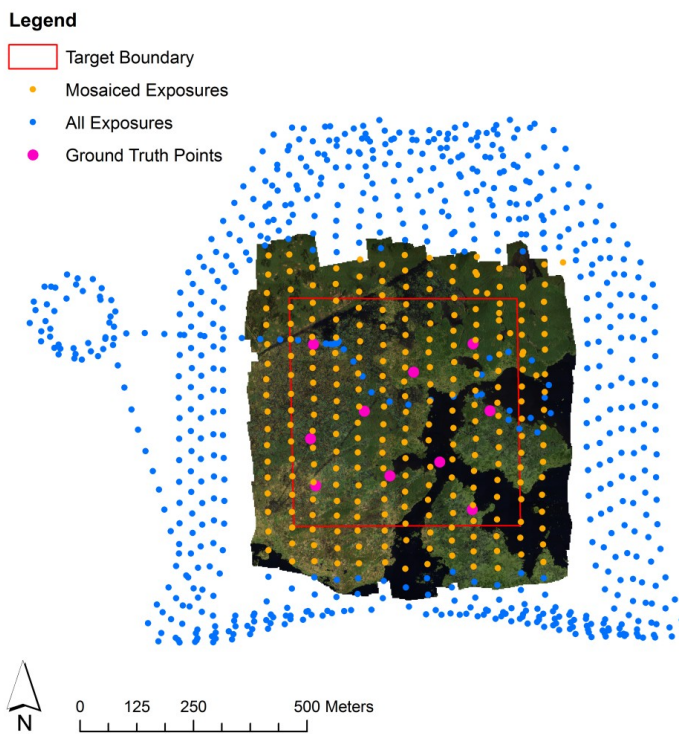


**Figure 3.** *Overview map of Phase 1*

## DATA PROCESSING

### *Preparation*

A total of 248 individual images were used to compose the mosaic, consisting of all images which were taken during stable flight at altitude and within a 100m buffer of the target area. The direct georeferencing parameters for each image were extracted by linear interpolation of the navigation data stream based on the synchronization data provided by the Burredo. This process is accomplished using a custom Python script that parses the log file accompanying the data set. The direct georeferencing parameters were converted to exterior orientation parameters by applying a coordinate axis transformation. Boresight parameters were not applied to the data set

given a lack of calibration data. Leverarm corrections are more than an order of magnitude less than the overall accuracy of the navigation system, precluding the necessity of their use. Due to flight planning, all images included in the mosaic were within  $15.75^\circ$  in the kappa, minimizing the relative rotation between images.

## Results

The automatic tie point generation process produced a cloud of 2,333 tie points. Image matching was performed on the red color band. 14,573 individual image observations were made, for a mean of 6.2 observations per tie point. Of these, 59 observations were rejected as blunders during the robust estimation procedure, with 3 tie points subsequently rejected due to insufficient observations. Among tie points that fell within the target area, the average number of observations was 7.4 (see Figure 4).

The self-calibrating bundle adjustment yielded a standard deviation of unit weight of  $S_0 = 1.078$ . A priori estimates of the accuracy of the directly georeferenced exterior orientation parameters were derived from the manufacturer's specifications. The focal length and pixel size were given by nominal values provided by the camera manufacturer, and the interior orientation parameters were included in the adjustment procedure. A simple two parameter, fourth-order radial lens model was included for lens distortion. The self-calibration parameters are given in Table 1.

Of significant interest was the post-adjustment accuracy of the object space coordinates of the ground points, a strong indicator of the geometric accuracy of the map. The estimated tie point mean horizontal RMSE was 11.5 cm, mean vertical RMSE was 9.1 cm, and mean positional RMSE was 14.7 cm for tie points that fell within the target area (see Figure 6). The distance from the centroid of the adjustment was highly correlated to the object space accuracy of the tie points. The steep bowl shape observed in Figure 7 is strong justification for using a coverage buffer around the target that includes a minimum of one additional flight line, as was done for this data set.

Parameter	Value	RMSE (mm)
$f_c$	24.9441	.0108
$x_0$	-0.0607	0.0072
$y_0$	-0.0348	0.0072
$k_1$	$-2.7441e^{-4}$	$1.5835e^{-6}$
$k_2$	$1.0122e^{-7}$	$1.4670e^{-8}$

**Table 1.** *Adjusted interior orientation parameters*

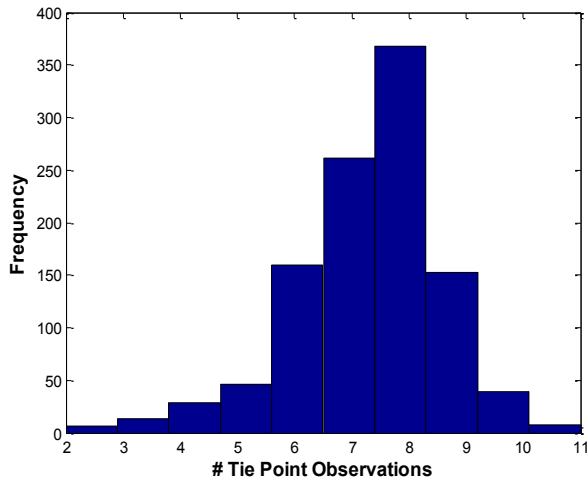


**Figure 4.** Histogram of tie point observation redundancy

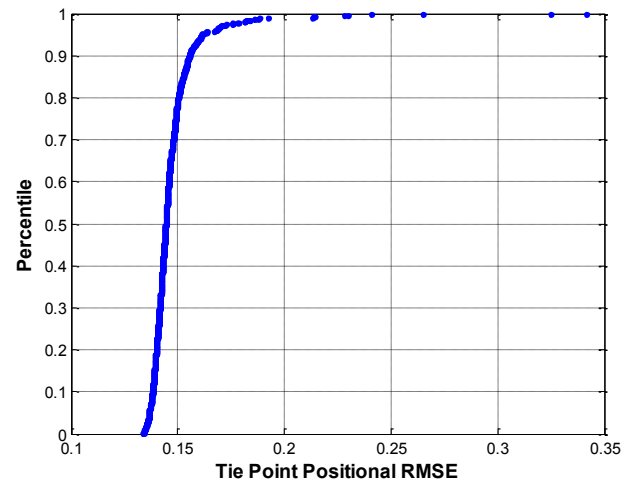


**Figure 5.** The effective cumulative distribution function of the target area's tie point positional RMSE

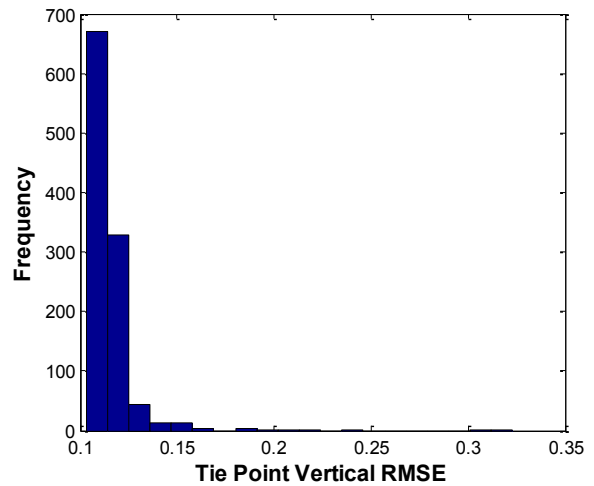
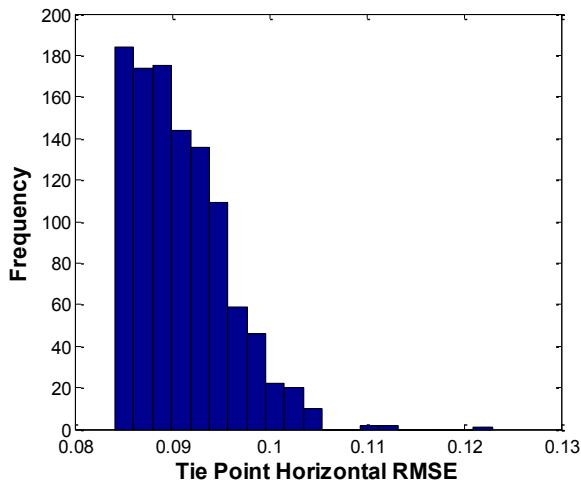


**Figure 6.** Histogram of the target area's tie point horizontal (left) and vertical (right) RMSE

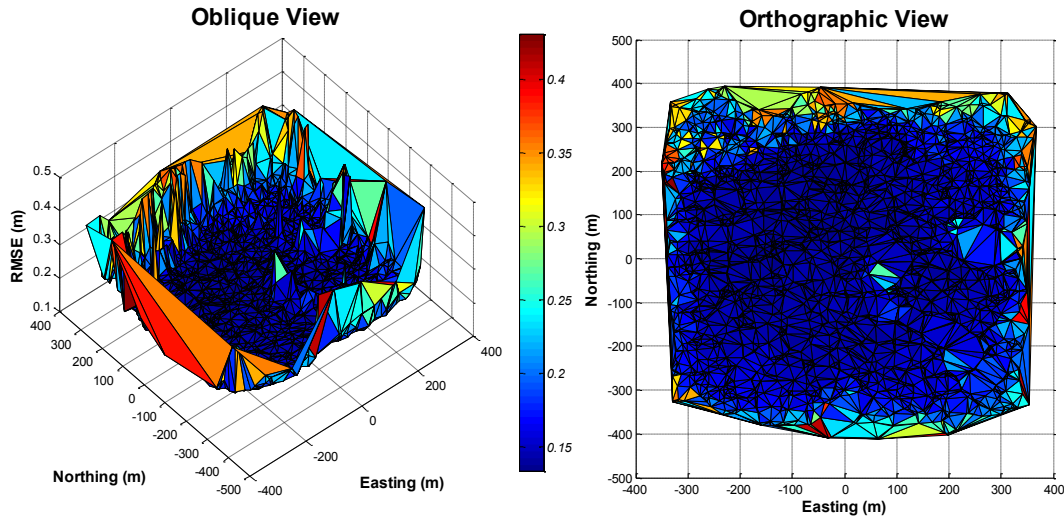


**Figure 7.** *Perspective and orthographic views of the surface created by the tie point positional RMSE. The geographic distribution of the error surface shows an obvious increase in the uncertainty toward the edges of the mosaic, and smaller peaks in the center-right area corresponding to areas of open water.*

The exterior orientation parameters and their adjustment residuals were analyzed for biases. In particular, the orientation parameters were expected to show a biased residual due to an imprecise boresight calibration. This is an ongoing concern, since the use of biased directly georeferenced EOPs is a violation of the underlying assumptions of the bundle adjustment. The data (see Figure 8) suggest a bias of approximately  $0.5^\circ$  on the  $\omega$  and  $\phi$  axes, although it is not conclusive. For near-vertical images, the  $\kappa$  parameter is nearly equal to the heading. Due to the relatively poor observability of heading, it is expected to be worse than tilt. This result is observed in the data, as seen in Figure 8. The distribution of the RMSE associated with the adjusted position and orientations are shown in Figure 9. Notably, all of the observed time-dependent trends appear to be trending toward zero, suggesting that the directly georeferenced parameters may be capable of significantly better performance given better initialization procedures and more precise boresight calibration.

The final mosaic was produced using a pixel-similarity weighted seamline algorithm. The output ground sample distance was 5cm using a bilinear resampling function. The calculated maximum resolution attainable by the data set was 3.7 cm. The imagery was rectified using a DSM generated from the data set. The DEM extraction algorithm was seeded with the tie points. The entire 248-image orthomosaic was 236 megapixels in size, and the orthomosaic clipped to the target area was 100 megapixels. The output was in IMAGINE raster format, and the output coordinate system was the UTM Zone 17N projection of the WGS84 ellipsoid.

Without ground control data, it is not possible to provide a firm estimate of the absolute mapping accuracy. However, based on the statistical results of the bundle adjustment, this method

certainly meets or exceeds the spatial accuracy requirements of this mission, and the data from Phase 1 does not require further processing.

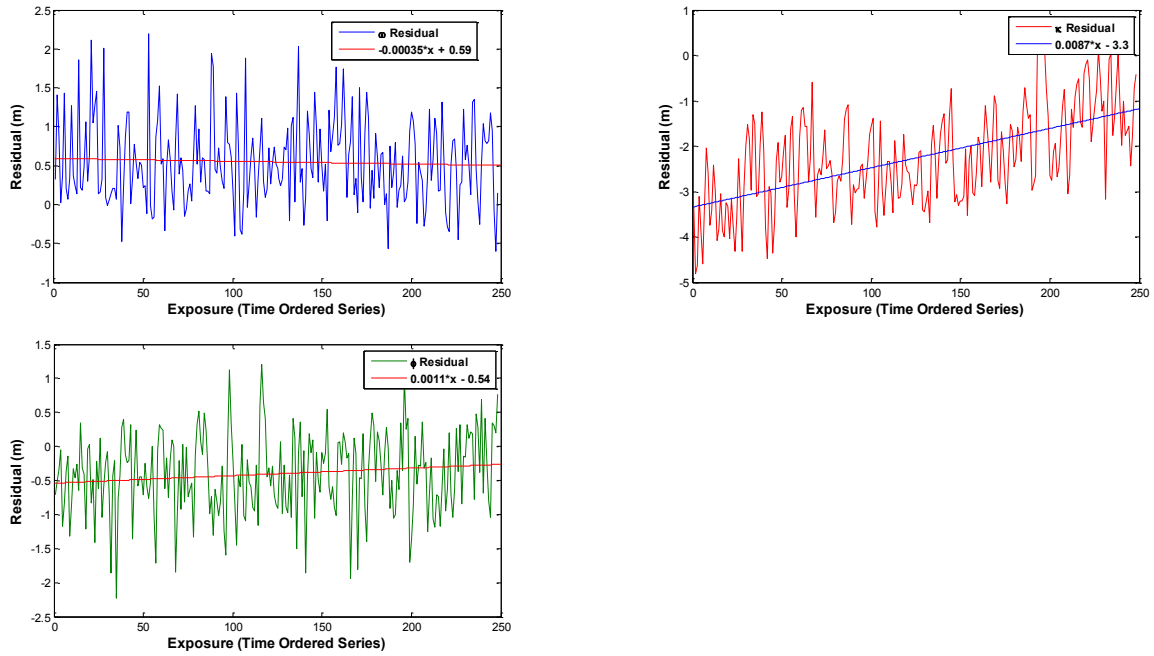


**Figure 8.** Residual plots of the  $\omega$  (top left),  $\phi$  (left), and  $\kappa$  (above) fitted with a linear model.

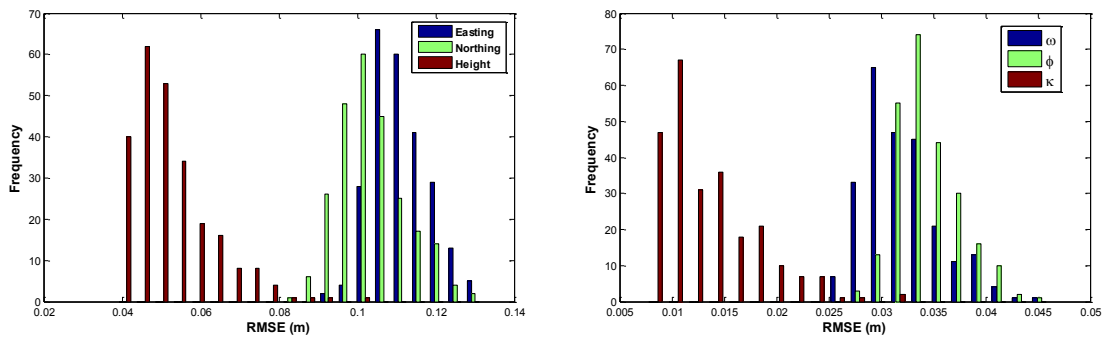


**Figure 9.** Histogram of the RMSE of the position (left) and orientation (right) of the camera at the time of exposure

## DATA ANALYSIS

### *Summary*

The primary goal of the first phase of data analysis is to develop an estimate for the composition of the local aquatic vegetation community. American lotus (*Nelumbo lutea*), frog's bit (*Limnobiium spongia*), American cupscale grass (*Sacciolepis striata*), exotic rice grass (*Luziola subintegra*), water lettuce (*Pistia stratiotes*), and water hyacinth (*Eichhornia crassipes*) were identified as the dominant vegetation species in the plot. A supervised classification of the scene (Figure 10) was conducted using ENVI from ITT Visual Information Solutions, Inc. In order to aid in the visual identification of the plant communities, the scene was transformed using a forward principal component transformation. A straightforward maximum likelihood classifier was used with the red, green, and blue channels as factors. The result of the classification is summarized in Table 2 and shown in Figure 11.

Several interesting effects are apparent in the classified images, such as the tendency of water lettuce to colonize immediately adjacent to open water. Similarly, the effect of previous herbicide treatment can be seen, as can the encroachment pattern of luziola into cupscale communities. A notable result is the presence of submerged or emergent decomposing vegetation, likely due to previous treatments, estimated to cover more than a quarter of the total surface area.

The classification performed on the imagery was rudimentary, and further classification efforts should be conducted using more factors and better algorithms to fully exploit the data. In addition, a statistical analysis of the classification has not been conducted. These results are expected in the associated Data Analyst report.

Class	Subclass	Area (m <sup>2</sup> )	% Total	% Class
Water		69,993	28%	
	Open Water	50,281	20%	72%
	Decomposing (Submerged)	19,712	8%	28%
Vegetation		180,007	72%	
	Frog's Bit, Water Hyacinth, & Cupscale	46,944	19%	26%
	Decomposing (Emergent)	45,889	18%	25%
	Water Lettuce	29,599	12%	16%
	Luziola	26,386	11%	15%
	Lotus	22,433	9%	12%
	Shadow/Unclassified	8,757	4%	5%
Total		250,000		

**Table 2.** Result of the supervised classification of the target area using the Phase 1 orthomosaic

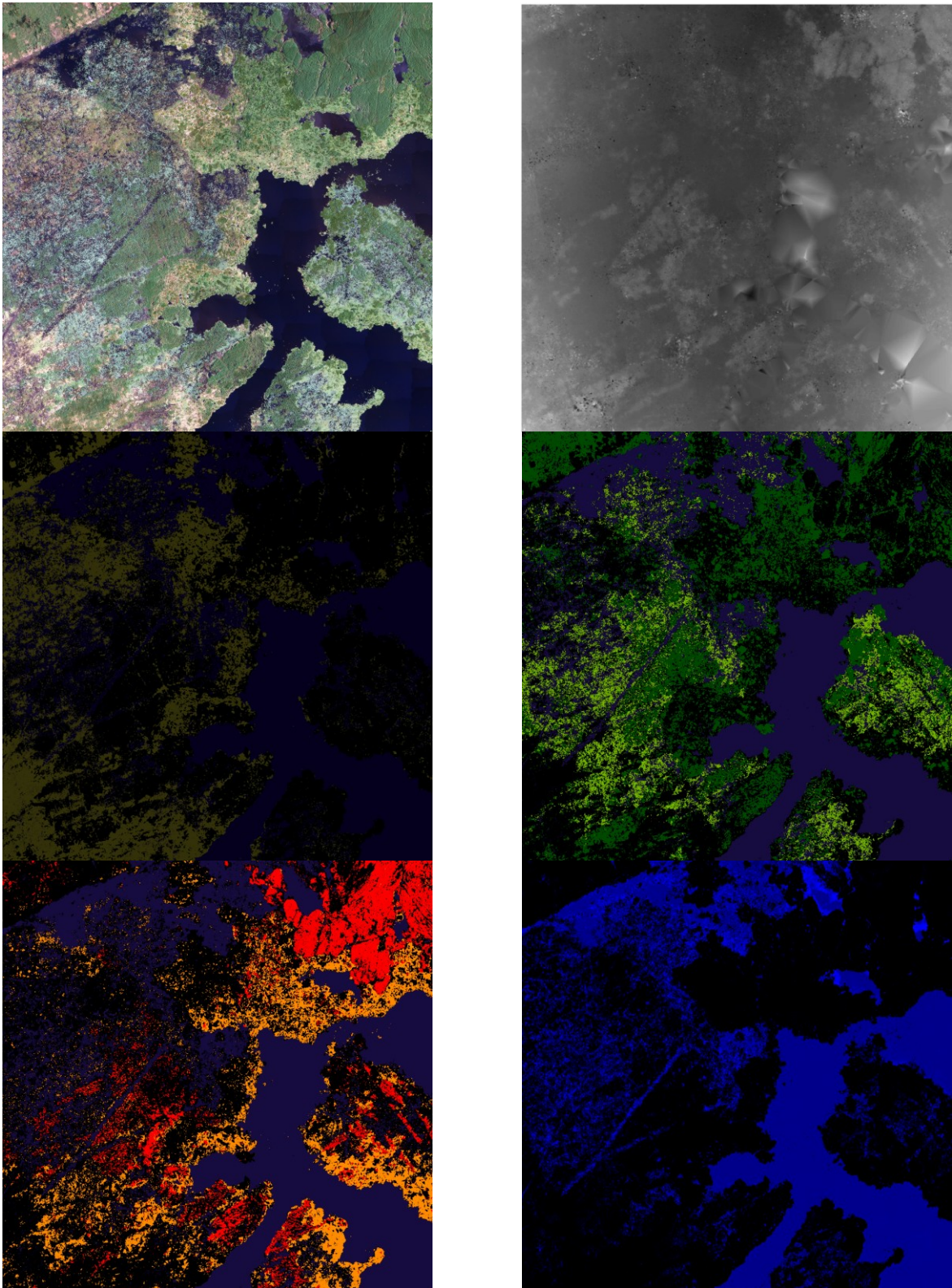


**Figure 11.** *Panchromatic orthomosaic (top-left), Photogrammetric DEM (top-right) decomposing emergent vegetation (mid-left), live native vegetation (mid-right), live invasive vegetation (bottom-left), and water including submerged decomposing vegetation (bottom-right)*

## Phase 2

---

### DATA ACQUISITION

#### *Flight Plan*

On September 18, 2010, two panchromatic payload flights and one near-infrared (NIR) flight was conducted at 200 m altitude over the 0.25 km<sup>2</sup> area designated in Phase 1. The coordinates of the target area were identical to Phase 1. Significant changes to the flight plan were required both before and during the field deployment in response to rapidly changing weather conditions as Tropical Storm Nicole passed within 100 miles of the target area 24 hours previous to flight operations.

Flight planning conducted by Matthew Burgess during Phase 1 relied on prevailing wind conditions from the south and east as is typical for the season. The passing storm instead drew winds from the west and northwest. Upon arrival at the site, the first flight was flown using the prepared eastward flight plan. With a windspeed of 5 m/s, upwind and downwind overlap met specification for the data set. However, the wind direction induced crab angle in excess of 20° along target flight lines. To ensure sufficient data acquisition, the flight crew in conference with Larry Taylor and Jon Morton agreed that a second flight was warranted. Thomas Rambo prepared a second flight plan, oriented north-northwest, and the area was reflown in the second panchromatic flight.

Finally, using the newly created flight plan, a near-infrared payload was flown over the target area. This data is not included in the official mission scope, and will be evaluated independently on an evaluation basis for future USACE missions.

#### *Equipment*

The panchromatic data (both flights) were captured using the U.S. Army Corps of Engineers' NOVA 2.1 UAS platform, configuration #1033. The imaging sensor was an Olympus E-420 dSLR camera, serial #G20519872, with a Zuiko 25mm lens, serial #292029187. The navigation system was the Xsens MTi-G integrated GPS/INS, serial #00500702, with Antcom antenna model #1G1215A-18NRS-4, serial #194292. Sensor synchronization was provided by the Burredo v4, serial #02.

The NIR data were captured using NOVA 2.1 UAS platform, configuration #1032. The imaging sensor was a modified Olympus™ E-420 dSLR camera, serial #50216725, with a Zuiko 25mm lens, serial #292027053, with a B+W™ 48mm #093-IR filter. The navigation system was the Xsens® MTi-G™ integrated GPS/INS, serial #00500702, with Antcom® antenna model #1G1215A-18NRS-4, serial #194292. Sensor synchronization was provided by the Burredo v4, serial #02.

## *Data Set*

The first RGB payload flight time was 8:54 AM – 9:32 AM, and total duration over the target area was 11.5 minutes. Linear flight length was 34 km. A total of 885 images were captured during the flight, yielding 3.20 GB of data in dataset ID# 30-09-2010-21-48-07. Images were recorded at a resolution of 3648 by 2736 (9.98 megapixels) with 8 bit per channel RGB using JPEG compression. Exposures were 1/2000<sup>th</sup> speed, f-stop 2.8, and ISO-100. Nominal focal length was 25mm, with a nominal forward and side field of view of 40° and 30°, respectively. Nominal flight line spacing was 50m. Mean airbase was 51.8 m between adjacent photographs along the flight line, with a mean exposure interval of 2.32 seconds. As noted in Phase 1, delays in the exposure interval are highly correlated to open water, and indicate the inability of the automatic focusing and metering system to function over featureless terrain. Nominal altitude was 200m, with a mean altitude of 201.5 m. The foregoing values were using direct exterior orientation parameters.

The second RGB payload flight time was 11:07 AM – 11:50 AM, and total duration over the target area was 19.6 minutes. Linear flight length was 36 km. A total of 1010 images were captured during the flight, yielding 3.78 GB of data in dataset ID# 30-09-2010-23-58-45. Images were recorded at a resolution of 3648 by 2736 (9.98 megapixels) with 8 bit per channel RGB using JPEG compression. Exposures were 1/2000<sup>th</sup> speed, f-stop 2.8, and ISO-100. Nominal focal length was 25mm, with a nominal forward and side field of view of 40° and 30°, respectively. Nominal flight line spacing was 50m. Mean airbase was 34.7 m between adjacent photographs along the flight line, with a mean exposure interval of 2.27 seconds. Nominal altitude was 200m, with a mean altitude of 202.7 m. The foregoing values were calculated using direct exterior orientation parameters.

The NIR payload flight time was 12:33 PM – 1:22 PM, and total duration over the target area was 19.6 minutes. Linear flight length was 36 km. A total of 1194 images were captured during the flight, yielding 3.78 GB of data in dataset ID# 30-09-2010-23-58-45. Images were recorded at a resolution of 3648 by 2736 (9.98 megapixels) with 8 bit per channel RGB using JPEG compression. Exposures were 1/1000<sup>th</sup> speed, f-stop 2.8, and ISO-100. Nominal focal length was 25mm, with a nominal forward and side field of view of 40° and 30°, respectively. Nominal flight line spacing was 50m. Mean airbase has not been determined at this time, with a mean exposure interval of 2.47 seconds. Limitations of the camera hardware forced a modification of the NIR system's autofocus system, allowing refocusing only once every ten exposures. The exposure interval increased approximately 22% during refocusing. Nominal altitude was 200m, with a mean altitude of 202.7 m. The foregoing values were calculated using direct exterior orientation parameters.

## Resources

Data processing was performed by John Perry and Damon Wolfe on October 5<sup>th</sup> through 7<sup>th</sup>. The ratio of data acquisition time to processing time was in excess of 1:100, including unattended compute time. This figure was reflects the processing of the largest data set ever attempted (combining both the first and second panchromatic flights into a single adjustment), as well as the ongoing training and development of the processing workflow.

The following software packages were used to process the data. The Leica Photogrammetry Suite™ (LPS) from ERDAS, Inc., including the auxillary software modules for terrain extraction, radiometric correction, and mosaicing, were used for the photogrammetry stages of the workflow. ArcGIS from ESRI, Inc. was used to interactively subset the data during the preprocessing stages, and the output of the processing workflow was targeted for this platform. Statistical and geometric analysis of the processing results was performed using Microsoft Excel and MatLAB from The Mathworks, Inc.

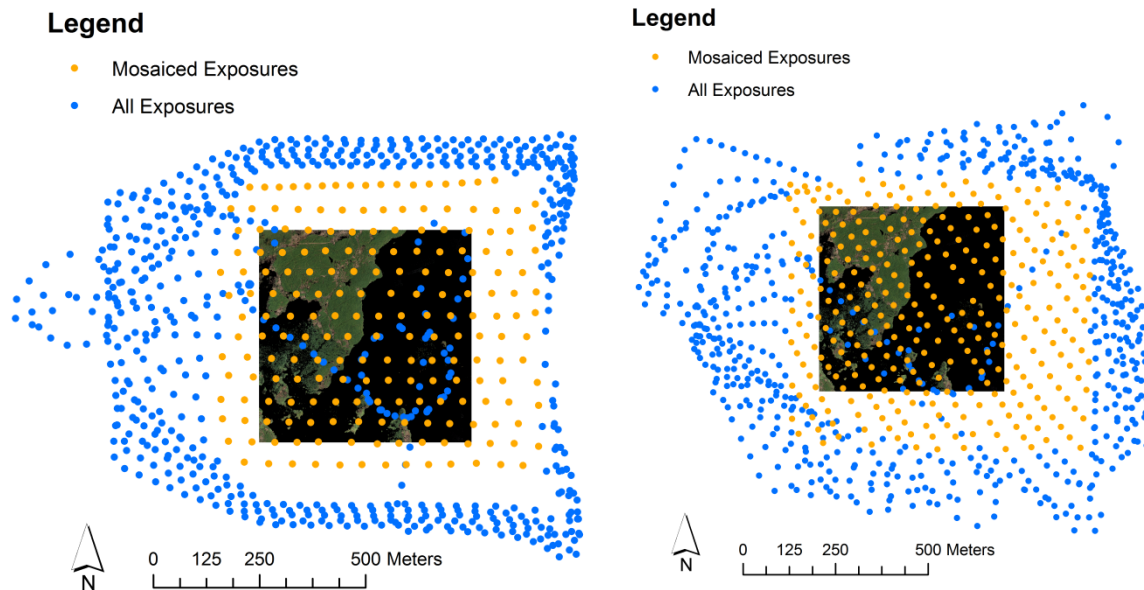


**Figure 12.** Overview map of Phase 2, RGB payload flight 1(left) and flight 2 (right)

## DATA PROCESSING

### *Preparation*

A total of 507 individual images were used to compose the mosaic, consisting of all images which were taken during stable flight at altitude and within a 100m buffer of the target area from both panchromatic payload flights 1 and 2. Preprocessing of the data followed an identical procedure as in Phase 1. Due to weather conditions, images from the first flight had crab angles exceeding 20°. Variable winds contributed to an overall standard deviation of 7.8° in heading, and a roll standard deviation 3.5°.

### *Results*

The automatic tie point generation process produced a cloud of 6,911 tie points. Image matching was performed on the red color band. Due to large expanses of featureless terrain (open water), the geometry of the bundle adjustment solution was poor both within and outside the target area. Particularly near the shoreline, the seam line errors are noticeable and occasional gross errors on individual frames were observed. As images with poor feature distribution were removed from data set, these effects were reduced dramatically. In addition, the tie point density and target number for tie points per image were increased over typical values by 4x and 2x, respectively, in an attempt to improve tie point redundancy in the scene.

Although the bundle adjustment converged with valid a priori standard deviations, the posteriori statistics indicated a poor overall solution, with a standard deviation of unit weight of 11.47. Despite the relatively poor indicators, time constraints pressed the production of a mosaic, which was then evaluated based on mosaicing seam error. Based on a sample of 10 measureable points along the seam, the seam line error had a RMSE of 0.72 meters.

The final mosaic was produced using a nearest-nadir seam line algorithm using only images from Flight 1 (Figure 13). The output ground sample distance was 5cm using a bilinear resampling function. The calculated maximum resolution attainable by the data set was 4.4 cm. The imagery was rectified using a flat surface model calculated from the mean elevation of the tie point cloud, -25.2 meters on the WGS84 ellipsoid. No DEM was extracted. The entire orthomosaic was 311 megapixels in size, and the orthomosaic clipped to the target area was 100 megapixels. The output was in IMAGINE raster format, and the output coordinate system was the UTM Zone 17N projection of the WGS84 ellipsoid.

Without ground control data, it is not possible to provide a firm estimate of the absolute mapping accuracy. Based on the statistical results of the bundle adjustment, the data has not been fully adjusted. However, the data does meet the accuracy requirements of the project and can be used to accurately quantify the scene's vegetation communities as well as support the change analysis from phase 1.

## DATA ANALYSIS

### *Summary*

The primary goal of the second phase of data analysis is to evaluate the overall change in vegetation composition of the scene. Using a maximum likelihood classifier under the same methodology as Phase 1, the most significant result found was that the herbicidal treatments have resulted in a reduction of total vegetation coverage from 70% to 30%. Further classification of the vegetation will be presented in the Data Analyst report, scheduled for release at a later date (see Figure 13). Visual inspection of the data indicates that both water lettuce and water hyacinth populations have been decimated, with total coverage estimated to be less than 2%. The dominant vegetation species are cupscale and luziola with a small community of water lotus.

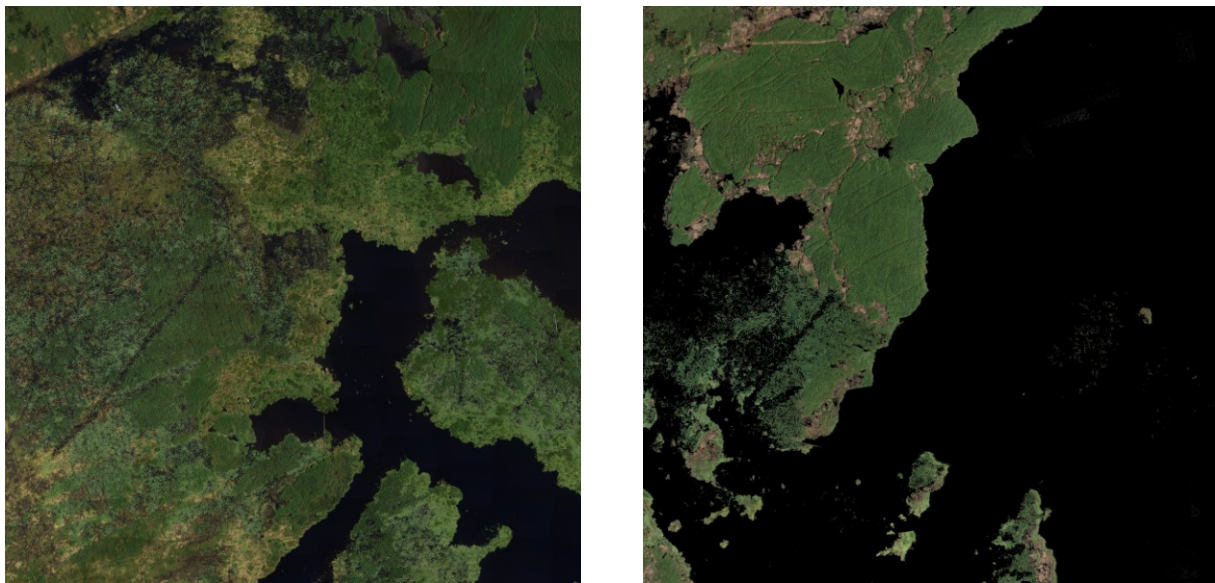


**Figure 13.** *Pre-treatment (left) and post-treatment (right) orthomosaics of the target area.*